Kink switching in ferroelectric free-standing films with high spontaneous polarization

E.I. Demikhov
Institute of Physical Chemistry, University of Paderborn, 33095 Paderborn, Germany

S.A. Pikin
Institute of Crystallography, Russian Academy of Sciences, 117333 Moscow, Russia

E. S. Pikina
Institute of Oil and Gas Problems, Leninsky Prospect 63, 117917 Moscow, Russia
(Received 28 July 1995)

The dynamics of a Sm-C^* director field in an a.c. electric field has been studied by means of light scattering. The scattering of resonance type has been observed by the variation of field frequency at fixed temperatures. The resonance scattering is supressed in high electric fields, at low temperatures in the Sm-C^* phase, and in films thinner than a threshold value N_0. A theory of director switching is proposed that consistently describes the observed anomalies. The film parameters viscosity, dielectric anisotropy, and polar film anisotropy are determined. This work provides evidence that the Sm-C^* structure in the boundary layers and the thin films of materials with high spontaneous polarization correspond to the weak anisotropic state predicted early.

PACS number(s): 64.70.Md, 68.15.+e

I. INTRODUCTION

Free-standing smectic films have recently experienced a period of renewed interest because of the unique properties that make them a very convenient experimental and theoretical object for studies of dimensional crossover effects and physics of liquids with confined dimension [1,2]. Until recently, the investigations of free-standing films have been restricted by achiral and low spontaneous polarization smectic phases. Qualitatively, new properties have been recently observed in ferroelectric films with high spontaneous polarization. It has been shown that the value of spontaneous polarization influences the phase diagram and the structure of chiral phases [3–8]. In thick films, a flexoelectric stripe instability has been observed, whereas in thin films a spontaneously anisotropic state is formed. All experimental results known until now show that the structure of the Sm-C^* phase in thin films with high spontaneous polarization ($N \leq 120$) corresponds to the weak anisotropic state of two-dimensional (2D) ferroelectric films predicted in [9,10]. In this case, the Sm-C^* layers should possess a long-range orientational order which occurs because the anomalous thermal fluctuations are suppressed by the electrostatic dipolar interaction.

There is a well-known correlation between the structure of ferroelectric phases and the dynamics of the director field in an electric field. Director field dynamics in free standing films with high spontaneous polarization has not been investigated, to the best of our knowledge. The aim of this work is to study the director switching processes in Sm-C^* free-standing films with high spontaneous polarization and to prove the structure assignments for the Sm-C^* phase made in previous works. We have observed anomalous dynamic behavior of free-standing Sm-C^* films which has been consistently interpreted by the model of kink switching [11,12]. This model assumes that, at the application of electric field $\vec{E}$, which is directed oppositely to spontaneous polarization $\vec{P}$, small areas of the film are reoriented in the first stage ($\vec{P}$ becomes parallel to $\vec{E}$ at short distance η near the film boundaries preserving the initial orientation of $\vec{P}$), and then such a sharply inhomogeneous perturbation with width η (the width of kink) runs through the initially homogeneous film. Thus, it is assumed the that boundaries of ferroelectric film produce the certain anisotropic conditions for the distribution of polarization. These results correlate with the assumption made earlier [3,6,7] that the structure of thin ferrolectric films of high spontaneous polarization Sm-C^* phase corresponds to the weak anisotropic state predicted in [9,10].

II. EXPERIMENTAL RESULTS

Chiral 4-(2S,3S)-2-[chloro-3-methylpentanoyloxy]-4-′heptyloxybiphenyl (C7) has been studied. This substance possesses the following liquid-crystalline phases: isotropic (62 °C), smectic A(54.6 °C), smectic C^* (43 °C), smectic G [14]. The spontaneous polarization in the smectic-C^* phase of pure chiral C7 varies between 130 and 290 nC/cm^2 with decreasing temperature [14]. The first order smectic-A–smectic-C^* phase transition disappears in free-standing films thinner than $N \approx 15$ layers [15].

Films of C7 with dimensions 0.8×1 mm^2 were drawn in a frame consisting of two teflon rails and two movable brass blades. Films with homogeneous thickness were produced in the smectic-A phase and cooled down to the smectic-C^* phase. The C7 free-standing film prop-

erties have been studied in a broad interval of number of layers (from 5 to 1000). The experimental setup enabled simultaneous optical observations and reflectivity measurements in the visible region of wavelengths. The number of smectic layers was determined by the optical diffraction measurements in the smectic-A phase as described in [1,16]. The applied method allows the exact determination of number of layers in a broad interval of film thicknesses and the refractive index [16].

The conventional dielectric spectroscopy cannot be applied to detect collective modes inherent for the films because of the large amount of the substance contained in the meniscus. To solve this problem, an optical registration method has been developed. A sine wave electric field from a function generator has been applied across the film between two brass blades in the Sm-C^* temperature interval. The blades were covered with polyimide to prevent effects of charge injection. The presence of currents was controlled in a polarized microscope because the charge flow destroy the films texture. The used current passivation method works no longer than 3-4 days. After this time the currents occurrence was registered. In this case, the experiments were stopped and a new coating produced. It was important to take care about the substance destruction in films. At normal conditions the C7 is very stable, but we have observed that this process is much more faster in the electric field. To prevent this effect we have loaded new substance each day. The films were illuminated by a halogen lamp or laser in slightly decrossed polarizers and the light beam was collimated to 600 μm. The reflected intensity has been registered by a photomultiplier connected to a lock-in at the frequency of the electric field. The generator frequency change and data acquisition in the range 10 Hz–100 kHz has been carried out by a computer program.

Figure 1 shows the reflection intensity as a function of the ac electric field frequency in the smectic-C^* phase at $(T_{ac}-T)$=0.5 °C in a C7 free-standing film with $N = 400$ layers. The intensity curve possesses a maximum at $f \approx$ 2.8 Hz and a half-width $\Delta f \approx 800$ Hz. The film's texture was homogeneous with a small number of defect lines going from one electrode to the other.

Figure 2 shows variation of the scattering curves on the number of layers. The resonance dependence of $N = 400$ layer film becomes broader in $N = 152$ layer film. In films thinner than 120 layers, the resonance reflectivity disappears. The scattered intensity on the $N = 50$ layer curve increases in the low frequency region. Microscopic observation shows that, at the same time, quasistatic (low frequency) defects are born. Such defects move with some small velocity across the films and cause the change of the scattered intensity. At low frequencies the scattered intensity becomes some chaotic function of frequency in the $N = 50$ film (not shown in Fig. 2). The quasistatic defects will be studied in a separate paper.

Figure 3 shows the dependence of the resonance frequency and amplitude on the ac electric field strength for $N \approx$ 300 and $(T_{ac} - T) \approx 0.55$ °C. The resonance frequency is approximately independent on the field strength whereas the amplitude runs through a maximum at about 60 mV/μm and decreases in higher fields.

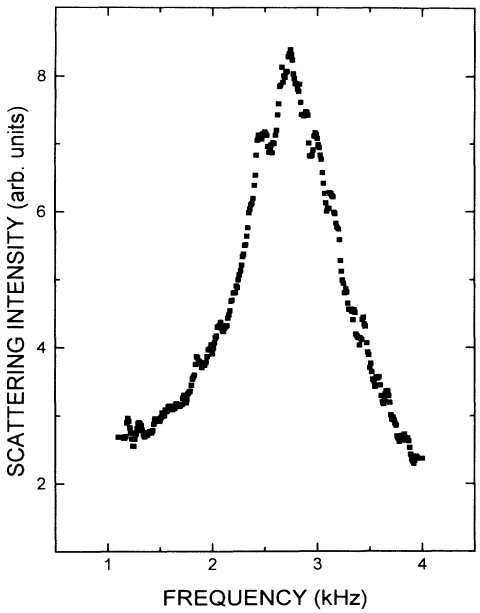

FIG. 1. Resonance reflectivity of a smectic-C^* with $N = 400$, $\Delta T = 0.5$ °C.

At $V \approx$170 mV/μm the resonance scattering disappears, which is shown on Fig. 4.

Figure 5 shows the dependence of the resonance frequency and amplitude on the offset field strength for the film with $N = 152$ layers. It is interesting that very small electric fields strongly influence the film properties. In higher dc fields the resonance scattering transforms to the step form and finally disappears. The resonance frequency has a maximum at approximately 8 mV/μm and decreases in higher dc fields. It is important to note that, because of the polyimide coating, the direct field induces only the reorientation of the molecular tilt planes and no currents. The amplitude of scattering remains approxi-

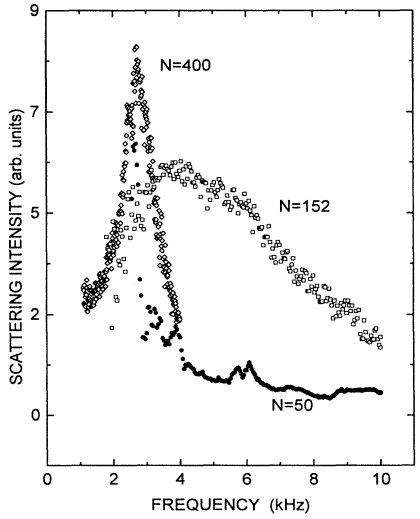

FIG. 2. Reflectivity curves for N=400 layers (◇), 182 layers (□), and 152 layers (•).

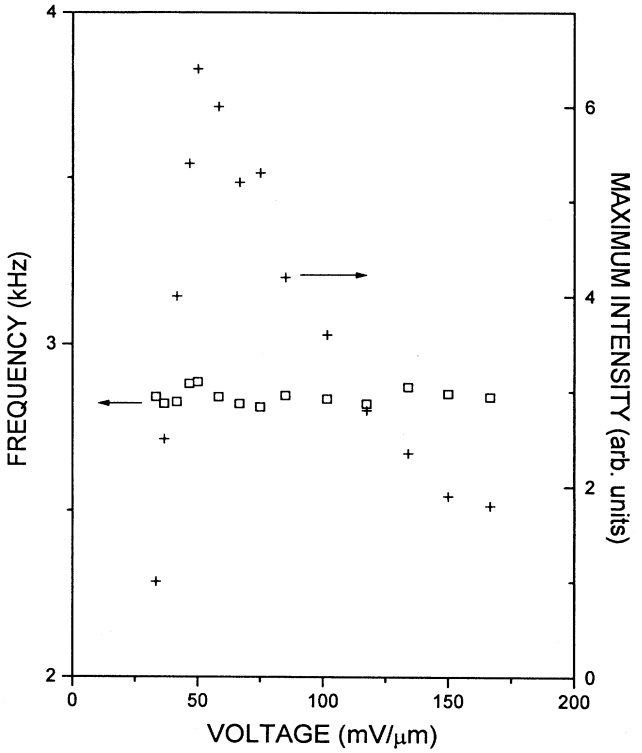

FIG. 3. ac field strength dependence of the resonance frequency (□) and amplitude (+) for $N = 300$ layer and ΔT=0.55 °C.

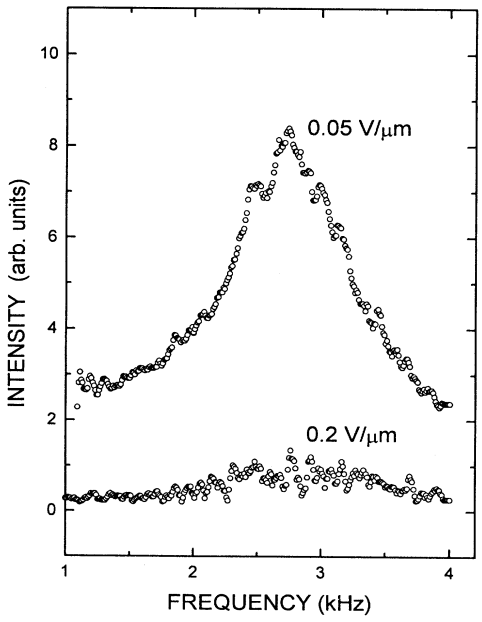

FIG. 4. Disappearance of resonance scattering in high ac electric field.

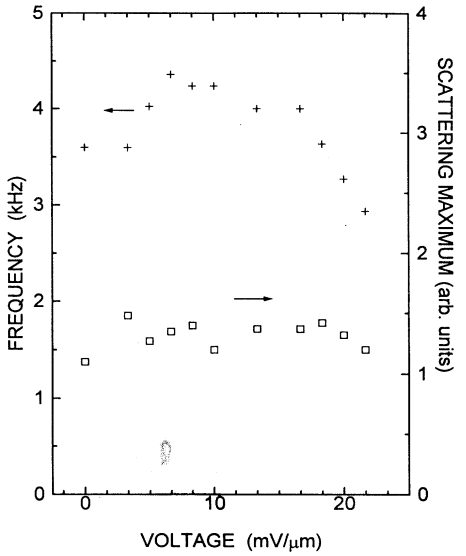

FIG. 5. Dependence of the resonance frequency (+) and amplitude (□) on the magnitude of bias field for $N = 152$ layers and ΔT=0.3 °C.

mately constant in increasing dc field.

Figure 6 presents the temperature dependence of the resonance frequency for different film thicknesses. In thick films ($N \geq 250$), the resonance frequency shows a maximum at the Sm-A–Sm-C^* phase transition and decreases with decreasing temperature. In films with number of layers $250 \geq N \geq 160$, the resonance frequency reveals a weak temperature dependence and slowly increases by lowering the temperature. In films with $160 \geq N \geq 120$, the resonance frequency increases by decreasing the temperature. The temperature interval, where the resonance reflection is observed, decreases by lowering the number of layers. In films thinner than 120 layers no resonance has been detected. The width of reflection curves, measured at a fixed temperature below T_{ac}, increases as the number of layers is decreased. In thick films, the stripe texture is stable in the electric field about 5 °C below the phase transition and frequencies $\omega \geq 500$ Hz. In thin films, the anisotropic texture was observed in field in the whole smectic-C^* temperature interval.

Figure 7 displays the dependence of the scattering amplitude for $N = 182$ and 152 layer films on temperature. Qualitatively different behavior was registered for this relatively small variation of the number of layers. The value of scattering maximum increases for $N = 182$ and decreases for $N = 152$ by decreasing the temperature.

III. THEORETICAL MODEL

In the geometry under consideration (Fig. 8), when the external electric field $\vec{E}$ is parallel to smectic planes and induces the polarization vector rotation by azimuth angle $\varphi(\vec{r}, t)$ in these planes, we can write the equation of director and polarization motion in the form [13]

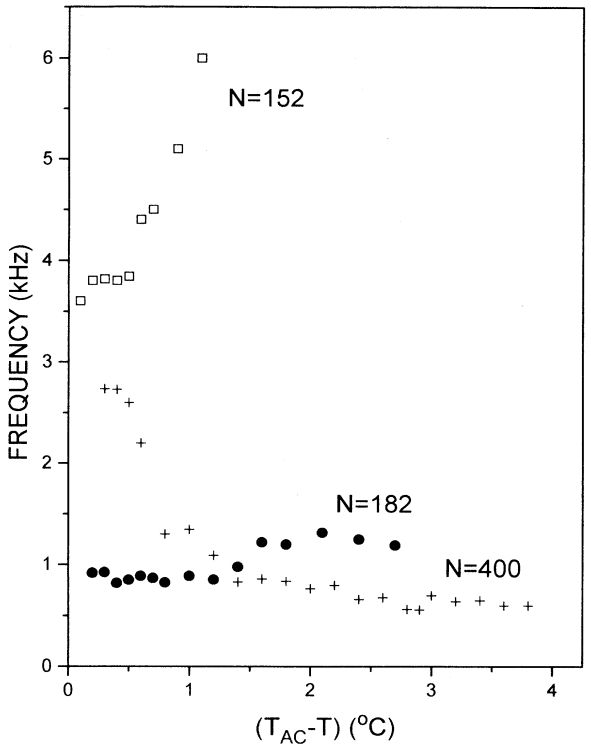

FIG. 6. Temperature dependence of the resonance frequency for $N = 400$ layers (+), 182 layers (•), and 152 layers (□).

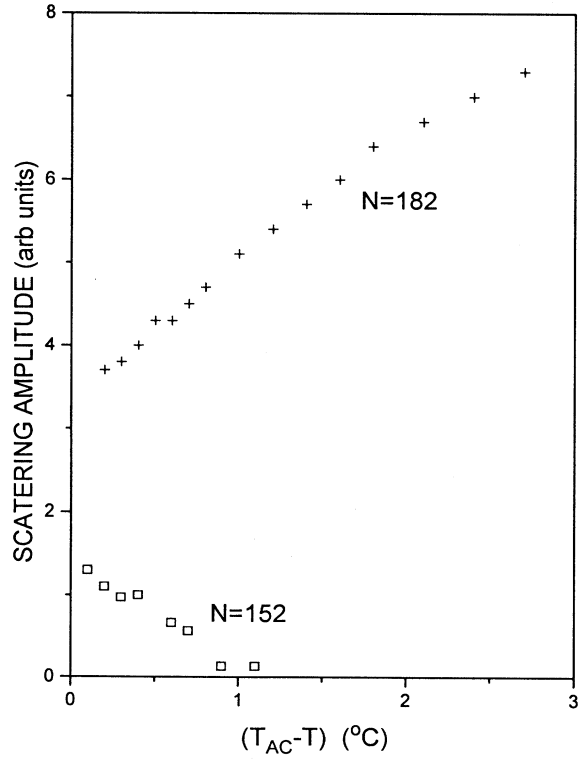

FIG. 7. Temperature dependence of the resonance amplitude for $N = 182$ (+) and $N = 152$ (□).

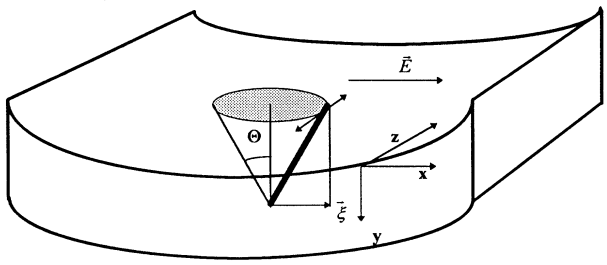

FIG. 8. Geometry of the film.

$$PE\sin\varphi - U\theta^2\sin\varphi\cos\varphi + K\theta^2\frac{\partial^2\varphi}{\partial y^2} = \gamma\theta^2\frac{\partial\varphi}{\partial t}, \quad (1)$$

where φ is the angle between vectors $\vec{P}$ and $\vec{E}$, $P = \mu\theta$ is the spontaneous polarization, θ is the tilt angle, μ is the piezoelectric modulus, K is the elastic constant, and γ is the viscosity coefficient. The quantity

$$U = U_0 + \epsilon_a E^2 \quad (2)$$

characterizes the energy of anisotropy [12,13], the quantity U_0 describes a possibility for the existence of preferential direction of the spontaneous polarization in the cell, for instance, due to boundary conditions, ϵ_a is the dielectric anisotropy. We shall assume that U is positive, i.e., the preferential orientations correspond to values φ=0 and φ=π. We suppose in Eq. (1) that angle φ changes along the y axis, which is perpendicular to the cell surfaces (any axis is suitable). The right part of Eq. (1) corresponds to the existence of the invariant expression

$$\gamma\left(\xi_1\frac{\partial\xi_2}{\partial t} - \xi_2\frac{\partial\xi_1}{\partial t}\right) = \gamma[\vec{\xi}\times\dot{\vec{\xi}}]_y \quad (3)$$

for the viscous torque which hinders the rotation of vector $\vec{\xi}$ with components

$$\xi_1 = \theta\cos\varphi\ , \quad \xi_2 = \theta\sin\varphi\ . \quad (4)$$

Here $\vec{\xi}$ is the order parameter of ferroelectric smectic C [10]. Equation (1) can describe a director motion under the action of alternating field $E = \tilde{E}\cos(\omega t)$ also, but, in such a case, we shall use the approximate expression for energy of anisotropy U,

$$U \approx U_0 + \epsilon_a\langle E^2\rangle = U_0 + \frac{\epsilon_a}{2}\tilde{E}^2, \quad (5)$$

which corresponds to the time averaging of U, the second harmonic in U being omitted. We think that such an approximation is sufficiently good for the qualitative model consideration.

It is convenient to introduce the variable $s = \frac{y}{\eta}$ and parameters

$$a = \frac{\mu\tilde{E}}{\gamma\theta}, \quad b = \frac{d}{\eta}, \quad \eta = \sqrt{\frac{K}{U}}, \quad (6)$$

where d is the cell thickness. One can find, under the

mentioned assumptions, the exact solution of Eq. (1),

$$\varphi(s,t) = \arctan \frac{1}{\sinh[s - s_0 - \frac{a}{\omega}\sin(\omega t)]}, \tag{7}$$

where s_0 is a constant. Solution (7) describes the solitary kink of function $\varphi(s,t)$ which is spreading along the y axis with velocity

$$v = \eta a \cos(\omega t). \tag{8}$$

If electric field E does not change with time t, i.e., frequency $\omega \Rightarrow 0$, then Eqs. (7) and (8) describe the kink motion

$$\varphi(s,t) = \arctan \frac{1}{\sinh(s - s_0 - at)} \tag{9}$$

with velocity $v = \eta a$ [11–13].

Solutions (7) and (9) demand, in fact, boundary conditions $\varphi = 0$ or $\varphi = \pi$ at very large values of

$$s - s_0 = \frac{(y - y_0)}{\eta}, \tag{10}$$

i.e., at very large kink displacements $y - y_0$ as compared with kink width η. In practice, the boundary conditions for the film with finite thickness d take, for example, the form

$$P\Phi \sin\varphi = K\theta^2 \frac{\partial\varphi}{\partial y} \tag{11}$$

at values $y = 0$ and $y = d$, where Φ is an effective electric potential of the cell surface. Taking into account the relation

$$\sin\varphi = \frac{1}{\cosh(s - s_0 - A)} = \eta\frac{\partial\varphi}{\partial y}, \tag{12}$$

$$A \equiv A(t) = \frac{a}{\omega}\sin(\omega t) \tag{13}$$

or

$$A(t) = at\ , \tag{14}$$

we conclude that condition (11) is equivalent to the condition

$$\frac{1}{\cosh(s - s_0 - A)} \Rightarrow 0 \tag{15}$$

at the cell boundaries. The latest condition is fulfilled approximately if kink displacements $|s - s_0| \sim |A| \sim \frac{a}{\omega}$ are much less than the parameter $b = \frac{d}{\eta}$ that is possible at large frequencies. In general, we will assume, by analogy with ordinary ferroelectrics, that the process of polarization reversal starts in certain "weak" places s_0 by the formation of nuclei which are the orientational kinks in our case. Such weak places can exist at the cell boundaries or in the bulk of the cell. If the time of nucleus (kink) formation is smaller than the characteristic time of kink displacements, then we can hope that solution (7) will describe the polarization reversal qualitatively. It is necessary to emphasize that we consider large reorientation angles $\varphi \sim \pi$; therefore this case differs from ordinary dielectric measurements in principle. Besides, one should note that we consider the polarization reversal among homogeneous orientational states, i.e., an orientational helix is absent in the case under consideration. Usually, in chiral ferroelectric smectics C, the helix is untwisted by the cell boundaries if the cell thickness d is sufficiently small, for instance, at $d < 0.1 - 1\ \mu$m.

The total intensity of scattering light is proportional to the integral of the scattering amplitude $\alpha(y,t)$ squared over variables y and t. The function $\alpha(y,t)$ is proportional to the quantity $\vec{i}\Delta\epsilon(y,t)\vec{f}$, where $\vec{i}$ and $\vec{f}$ are the initial and final polarizations of light, and $\Delta\hat{\epsilon}$ is the perturbation of the dielectric permeability tensor for a given light frequency. In the case under consideration, the quantity $\vec{i}\Delta\hat{\epsilon}\vec{f}$ is proportional to the difference of products of order parameter components

$$\xi_i(y,t)\xi_f(y,t) - \xi_i(y,0)\xi_f(y,0), \tag{16}$$

and therefore the scattering intensity is proportional to the quantity

$$I = \int_0^{\frac{2\pi}{\omega}} dt \int_0^d dy[\xi_i(y,t)\xi_f(y,t) - \xi_i(y,0)\xi_f(y,0)]^2. \tag{17}$$

According to the definition of components,

$$\xi_1(y,t) = \theta\cos\varphi(y,t),$$
$$\xi_2(y,t) = \theta\sin\varphi(y,t), \tag{18}$$

for the light incident on the cell along the y axis and for the electric field directed along the x axis, we can denote x for direction 1 and z for direction 2. If the light is polarized initially and finally along axis x, then we obtain quantity I_{11} from Eq. (17):

$$I_{11} = \theta^4 \int_0^{\frac{2\pi}{\omega}} dt \int_0^d dy[\cos^2\varphi(y,t) - \cos^2\varphi(y,0)]^2. \tag{19}$$

For the initial and final light polarizations directed along the z axis, we obtain the quantity

$$I_{22} = \theta^4 \int_0^{\frac{2\pi}{\omega}} dt \int_0^d dy[\sin^2\varphi(y,t) - \sin^2\varphi(y,0)]^2. \tag{20}$$

In the case of crossed polarizers, we have the quantity

$$I_{12} = \theta^4 \int_0^{\frac{2\pi}{\omega}} dt \int_0^d dy[\sin\varphi(y,t)\cos\varphi(y,t) - \sin\varphi(y,0)\cos\varphi(y,0)]^2\ . \tag{21}$$

Using the relations

$$\sin\varphi(y,t) = \frac{1}{\cosh(s - A)},$$
$$\cos\varphi(y,t) = \tanh(s - A),$$
$$\sin\varphi(y,0) = \frac{1}{\cosh s},\quad \cos\varphi(y,0) = \tanh s,$$
$$A \equiv A(t) = \frac{a}{\omega}\sin(\omega t),\quad b = \frac{d}{\eta}, \tag{22}$$

where the constant s_0 is omitted, which is not a factor, one can rewrite expressions (19)–(21) in terms of (22) and take integrals over coordinate y. For instance, we obtain

$$I_{22}(\omega)=\theta^4\eta\int_0^{\frac{2\pi}{\omega}}dt\Big\{\tanh b-\frac{1}{3}\tanh^3 b+\tanh A-\frac{1}{3}\tanh^3 A+\tanh(b-A)-\frac{1}{3}\tanh^3(b-A)$$
$$+\frac{2}{\sinh^2 A}\left[\tanh b+\frac{(1-\tanh^2 A)\tanh b}{1-\tanh b\tanh A}+\frac{2}{\tanh A}\ln(1-\tanh b\tanh A)\right]\Big\}, \tag{23}$$

$$I_{12}(\omega)=\theta^4\eta\int_0^{\frac{2\pi}{\omega}}dt\Big\{\frac{1}{3}\tanh^3 b+\frac{1}{3}\tanh^3(b-A)+\frac{1}{3}\tanh^3 A+\frac{2}{\sinh A}\ln(1-\tanh b\tanh A)$$
$$-\frac{2\cosh A}{\sinh^2 A}\left[\tanh b+\frac{(1-\tanh^2 A)\tanh b}{1-\tanh b\tanh A}+\frac{2}{\tanh A}\ln(1-\tanh b\tanh A)\right]\Big\}. \tag{24}$$

Integrals (23) and (24) cannot be expressed as elementary functions, and, besides, at very low frequencies ω, the limits of integration should be changed because of the following reasons. It is clear physically that when the period of electric field oscillations is much more than the time of kink motion through the cell, i.e., when $\frac{2\pi}{\omega}\gg\frac{d}{v}$, the perturbations of dielectric permeability occur during time $\frac{d}{v}$ only, and, therefore, in low frequency limit, when $A(t)\approx at$, we must take the integrals over time t between the limits 0 and $\frac{b}{a}$. In fact, quantities $I(\omega\Rightarrow 0)$ tend to finite limits effectively. At very high frequencies ω, when the amplitudes of kink oscillations are of the order of $\frac{\eta a}{\omega}$, i.e., they are much less than cell thickness d, intensities I must diminish. The decay $I(\omega\Rightarrow\infty)$ can be calculated exactly by the expansions in terms of quantity A. For example, from (23) and (24), we obtain

$$I_{22}(\omega\Rightarrow\infty)\approx\theta^4\eta(\tfrac{4}{3}\tanh^3 b-\tfrac{4}{5}\tanh^5 b)\left(\frac{\pi a^2}{\omega^3}\right), \tag{25}$$

$$I_{12}(\omega\Rightarrow\infty)\approx\theta^4\eta(6\tanh b-7\tanh^3 b+\tfrac{16}{5}\tanh^5 b)\left(\frac{\pi a^2}{\omega^3}\right). \tag{26}$$

From Eqs. (26) and (26), at small values of parameter b, we can estimate also the limits $I(\omega\Rightarrow 0)$ by the substitution

$$\int_0^{\frac{2\pi}{\omega}}A(t)^2dt=\frac{\pi a^2}{\omega^3}\Rightarrow a^2\int_0^{\frac{b}{a}}t^2dt=\frac{b^3}{3a}, \tag{27}$$

i.e.,

$$I_{22}(\omega\Rightarrow 0,b\Rightarrow 0)\approx\frac{4\theta^4\eta b^6}{9a}, \tag{28}$$

$$I_{12}(\omega\Rightarrow 0,b\Rightarrow 0)\approx\frac{2\theta^4\eta b^4}{a}. \tag{29}$$

Thus, one can see from Eqs. (25)–(29) that the limit values of quantity $I(\omega)$ are small at large values of parameter a (in practice, $a\sim 10^4$ sec^{-1}). At intermediate values of ω, we should expect the existence of a certain maximum in dependence $I(\omega)$. It is clear physically that maximum values of the scattering intensity must correspond to such a situation when the kink is running distance d during the time of the order of half-cycle $\frac{\pi}{\omega}$, because, in such a case, the perturbations of dielectric permeability are large anywhere in the bulk of cell. Thus, we can make the estimate

$$d\sim\frac{v}{\omega_{ext}}\sim\frac{\eta a}{\omega_{ext}}, \tag{30}$$

i.e.,

$$\omega_{ext}\sim\frac{a}{b},$$

frequency value ω_{ext} corresponding to intensity extremum $I_{max}=I(\omega_{ext})$.

The relation $\omega_{ext}\sim\frac{a}{b}$ can be obtained by the rough estimates of the integrals of $\tanh(b-A)$ and $\tanh^3(b-A)$ in expressions (23) and (24). It should be noted that the quantity

$$\theta^2\eta\int_0^{\frac{2\pi}{\omega}}\tanh(b-A)dt=\theta^2\eta\int_0^{\frac{\pi}{\omega}}\left[\tanh\left(b-\frac{a}{\omega}\sin(\omega t)\right)+\tanh\left(b+\frac{a}{\omega}\sin(\omega t)\right)\right]dt \tag{31}$$

characterizes the integral change of $\xi_2^2=\theta^2\sin^2\varphi(y,t)$, i.e., of the square of the polarization component perpendicular to the electric field direction, since

$$\theta^2\int_0^{\frac{2\pi}{\omega}}dt\int_0^d dy(\sin^2\varphi)=\theta^2\eta\int_0^{\frac{2\pi}{\omega}}[\tanh(b-A)+\tanh A]dt$$
$$=\theta^2\eta\int_0^{\frac{2\pi}{\omega}}\tanh(b-A)dt. \tag{32}$$

Assuming the existence of unequalities $b\gg 1, a\gg 1$ and $1\geq(b-\frac{a}{\omega}+\frac{1}{2}b\omega^2t^2)>0$, one can estimate integral (31) as

$$\frac{b\theta^2\eta}{a}\left\{\pi+\int_{-\frac{\pi}{2}}^{\frac{\pi}{2}}\tanh\left[\left(b-\frac{a}{\omega}\right)+b(1-\cos u)\right]du\right\}$$

$$\approx\frac{d\theta^2}{a}\left\{\pi+2\int_0^{\frac{\pi}{2}}\tanh[b(1-\cos u)]du+2\sqrt{\frac{2}{b}\left(1-b+\frac{a}{\omega}\right)}\left(b-\frac{a}{\omega}\right)\right\}$$

$$\approx\frac{d\theta^2}{a}\left[2\pi-\frac{\text{const}}{\sqrt{b}}+2\sqrt{\frac{2}{b}}\left(b-\frac{a}{\omega}\right)\sqrt{1-\left(b-\frac{a}{\omega}\right)}\right]. \quad (33)$$

Expression (33) has a maximum at $(b-\frac{a}{\omega})=\frac{2}{3}$, i.e., $\omega_{ext}\sim\frac{a}{b}$, and the maximum of integral (31) is of the order of $\frac{d\theta^2}{a}$. The same estimates are true for the integral of $\tanh^3(b-A)$ and for integrals (23) and (24). Thus, we have:

$$\omega_{ext}\sim\frac{a}{b}\sim\frac{\mu\eta\tilde{E}}{\gamma\theta d}\sim\frac{\mu\tilde{E}}{\gamma\theta d}\sqrt{\frac{K}{U}},$$

$$I_{max}(\omega\sim\omega_{ext})\sim\frac{\theta^4\eta b}{a}\sim\frac{\gamma\theta^5 d}{\mu\tilde{E}}. \quad (34)$$

The numerical calculations of the integral change of ξ_2^2 and of integral scattering intensity I_{12} as functions of frequency ω are shown in Figs. 9 and 10 respectively, for the identical sets of parameters a and b (multipliers θ and η are fixed). One can see that these integral characteristics are very similar qualitatively: the increase of parameter $a\sim\tilde{E}$ results in the decrease of these characteristics at fixed thickness $d\sim b$; the increase of thickness $d\sim b$ results in the increase of them and in the decrease of ω_{ext} at fixed parameter $a\sim\tilde{E}$; values ω_{ext} and I_{max} are almost identical to the ones at the identical values of ratio $\frac{a}{b}$; function $I(\omega)$ has a plateau at low frequencies.

All these conclusions follow from analytic relations (34). Relations (34) show also that, at the fixed values of tilt angle θ, the field dependencies of quantities ω_{ext} and I_{max} are different if $U\sim\tilde{E}^2$, namely, ω_{ext} is almost constant, but $I_{max}\sim\frac{1}{\tilde{E}}$. At small values of amplitude $\tilde{E}$, one can see from Eqs. (28) and (29) that intensity I decreases, at least as $\tilde{E}^2$ at decreasing $\tilde{E}$, if $a\sim\tilde{E}$ and $\eta\sim\frac{1}{\tilde{E}}$. The temperature dependences of quantities ω_{ext} and I_{max} are determined by the temperature dependence of tilt angle θ. For example, ω_{ext} decreases but I_{max} increases at decreasing temperature T, i.e., at increasing tilt angle θ.

If in phase C^*, due to the strong influence of film surfaces, the "easy" direction for the spontaneous polarization arises in a thin cell along the z axis, then quantity U_0 must be negative and increase at the temperature decreasing. In this case, quantity U can vanish at a certain intermediate temperature, and, therefore, kink width η becomes infinite and parameter b is going to zero at this temperature. Thus we obtain, by the first of Eqs. (34), that quantity ω_{ext} must diverge at such a point, but quantity I_{max} must vanish at this temperature according to Eqs. (26)–(29).

When direct field E_0 and alternating field $\tilde{E}\cos(\omega t)$ are applied simultaneously, then solution (7) takes form

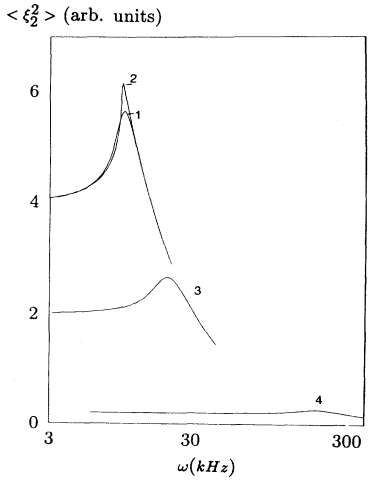

FIG. 9. The frequency dependence of the integral change of the square of the polarization component perpendicular to the direction of electric field. Numerical calculations: curve 1 ($a=10^4$ sec^{-1}, $b=10$); curve 2 ($a=10^5$ sec^{-1}, $b=10^2$); curve 3 ($a=10^5$ sec^{-1}, $b=10$); curve 4 ($a=10^5$ sec^{-1}, $b=1$). The value of $\langle\xi_2^2\rangle$ is plotted in arbitrary units.

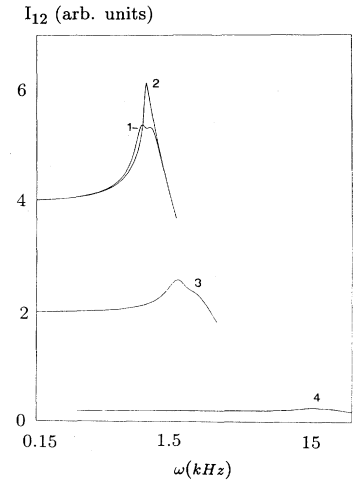

FIG. 10. The frequency dependence of the integral intensity of scattering for crossed polarizers. Numerical calculations: curve 1 ($a=10^4$ sec^{-1}, $b=10$); curve 2 ($a=10^5$ sec^{-1}, $b=10^2$); curve 3 ($a=10^5$ sec^{-1}, $b=10$); curve 4 ($a=10^5$ sec^{-1}, $b=1$). The value of I_{12} is given in arbitrary units.

$$\varphi = \arctan \frac{1}{\sinh[s \pm \delta a t - \frac{a}{\omega}\sin(\omega t)]}, \quad (35)$$

where $\delta = \frac{E_0}{\tilde{E}}$ and signs $\pm$ correspond to various mutual orientations of the two electric fields. If quantity E_0 is small, i.e., $\delta \ll 1$, then estimates (31)–(33) give a small shift of quantity ω_{ext} : $\omega_{ext} \sim \frac{a}{b}(1 + \frac{\delta^2}{2})$. At comparable values of E_0 and $\tilde{E}$, i.e., at $\delta \leq 1$, the situation can drastically change, since during one half-cycle, when vectors $\vec{E_0}$ and $\vec{\tilde{E}}$ have identical directions, the kink can rapidly run through the film and cannot come back, which decreases the scattering intensity. The perturbation occurs during sufficiently long time when these two fields are directed oppositely. In such a case, the characteristic frequency can be roughly estimated as

$$\omega_{ext} \sim \frac{(1-\delta)a}{b}, \quad (36)$$

i.e., the quantity ω_{ext} diminishes at $E_0 \simeq \tilde{E}$. The estimate of quantity I_{max} at these low frequencies can be done qualitatively for $b \gg 1$ by Eqs. (23) and (24) in which the integrals should be taken between the limits 0 and $t_0 < \frac{1}{\omega_{ext}}$, where time t_0 is an instrument constant. One can see that, at these conditions, the maximum intensity decreases in high fields as

$$I_{max} \sim \theta^4 \eta t_0 \sim \frac{1}{\sqrt{U}} \sim \frac{1}{\sqrt{E_0^2 + \frac{1}{2}\tilde{E}^2}}. \quad (37)$$

IV. DISCUSSION

The observed frequency dependence of the scattering intensity, shown in Fig. 1, reminds one of resonance behavior, but, in reality, the existence of a maximum intensity can be explained by the kink motion which was discussed above. Theoretically calculated functions $I(\omega)$ (see Figs. 9 and 10) are quite similar to the experimental ones. We fitted the observed dependence $I(\omega)$ at $\omega > \omega_{ext}$ by the law $G(\omega + B)^{-C}$; the fitting results are shown in Fig. 11. One can see that dependence $I(\omega) \sim \omega^{-3}$ is most suitable in accordance with Eqs. (25) and (26) parameter G being of the order of 10^8. It should be noted that, theoretically, $G \sim a^2$, and the theoretical curves were calculated for $a \geq 10^4$ sec^{-1}.

Figure 2 shows the experimental change of functions $I(\omega)$ as the film thickness decreases. The calculated curves, for parameter a = const and for parameter b decreasing, show a similar change: I_{max} decreases, but ω_{ext} increases.

Figures 3 and 4 show that I_{max} decreases, but ω_{ext} almost does not change; when the field amplitude increases at the constant tilt angle θ, this behavior is explained by Eqs. (34). Figure 3 shows also that, at low voltages, I_{max} increases with a voltage that agrees with Eqs. (28) and (29) when $a \sim b \sim \eta^{-1} \sim E$.

Figure 5 shows the experimental effect of bias field E_0 acting simultaneously with the alternating field. One can see that quantity ω_{ext} increases to some extent at low values of E_0, but then, at larger values of bias field, quantity ω_{ext} exhibits the essential decrease when E_0 becomes comparable with $\tilde{E}$. According to Eqs. (36) and (37) the magnitude of I_{max} should also decrease at these values of E_0. However, the data noise in Fig. 5 makes comparison with experiment difficult.

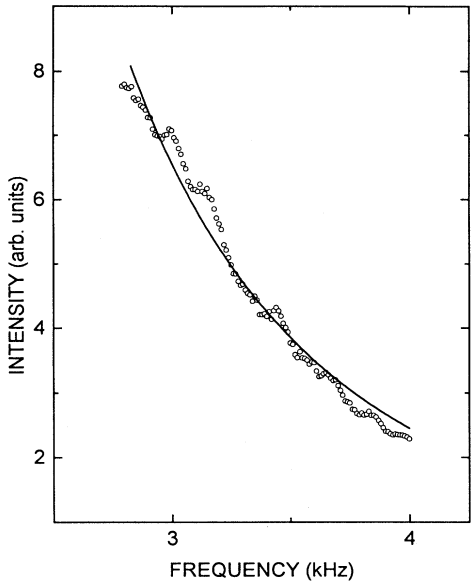

FIG. 11. Fitting of the high frequency wing of the scattering curve of Fig. 1.

Figures 6 and 7 display two kinds of the temperature dependences of quantities ω_{ext} and I_{max}. For the relatively thin film, we observed the vanishing of scattering and the critical increasing of ω_{ext} at a certain temperature below the transition temperature. For the thicker films, such a "critical" temperature is absent, quantity I_{max} increases, but quantity ω_{ext} decreases, with decreasing temperature. These data can be explained if we assume that there is no pronouced energy of polar anisotropy ($U_0 \approx 0$) in thick films, but there is the "easy" direction (z axis) for vector $\vec{P}$ in sufficiently thin films ($U_0 < 0$). Therefore, the pointed behavior of thick films is described by Eqs. (34), where quantity U is positive. The geometry of studied thin films can provoke the appearance of the "easy" z axis and of negative quantity U_0: the film is almost totally homogeneous along the z axis, whereas directions x and y correspond to inhomogeneous changes of film properties, for example, because of the influence of the film surfaces and electrodes. The temperature dependence of U_0 is determined by the fluctuational nature of the polar anisotropy: at the phenomenological approach, quantity U_0 is the expansion in terms of tilt angle squared, and we suppose that $U_0 \sim -\theta^2 \sim -(T_{ac} - T)$, so that the corresponding free energy term and the second term in Eq. (1) are proportional to θ^4. Thus, in this approximation, we can write

$$U = -\text{const} \times (T_{ac} - T) + \epsilon_a E^2 \quad (38)$$

where const is positive. This expression for the energy of

polar anisotropy results in the appearance of the "critical" temperature (for the effect under consideration) below the transition temperature as it was mentioned above. In our approach we used the linear relationship between P and θ. For the materials with high spontaneous polarization this is generally not true. It can be shown that the deviation from the linearity does not change the qualitative picture of the phenomena. The effects of nonlinear terms will be discussed in further publications.

Figures 9 and 10 show the computer simulation of the scattering curves on the number of layers and electric field according to Eq. (34) These curves demonstrate that the simulated curves qualitatively correspond to experimental behavior.

Since the kink motion is possible at values $b \gg 1$ only, i.e., when $d \gg \eta$, we conclude that, at the cell thicknesses smaller than 1μm and the field strength smaller than 10^6 V/m, the kink width could be larger than the cell thickness. Really, $\eta \sim \sqrt{K/\epsilon_a}\tilde{E}^{-1} \sim 10$ μm for $\tilde{E} \sim 10^5$ V/m, $K \sim 10^{-11}$ N, and $\epsilon_a \sim 10^{-11}$ m^2 N/C^2. Therefore, we should find the preferential direction for the kink formation and motion in plane xz, i.e., along the cell surface, with certain characteristic boundaries on distances $D \gg \eta$. In our experiments, such boundaries really exist as the boundaries of specific domains which were observed and studied [3–8]. Quantity D, as the width of the domains, is of the order of 100 μm. At very small film thicknesses ($d < 0.1$ μm), when these domains disappear, the time of kink motion becomes very long, if the latest one is not suppressed entirely by the cell boundaries, and, thus, we cannot expect any resonance phenomena.

To estimate the parameters of the kink model (a and b) and to fit the experimental data, we shall specify the characteristic quantities in the order of value as $\mu \sim 10^{-3}$ C/m^2, $K \sim 10^{-11}$ N, $\gamma \sim 10^{-1}$ Pa sec, $\tilde{E} \sim 10^5$ V/m, $D \sim 10^{-4}$ m, $\epsilon_a \sim 10^{-11}$ m^2 N/C^2, $U_0 = 0$ (for thick films) and $\theta \sim 10^{-1}$ at $\Delta T \sim 1$K. Thus, we can estimate $a = (\mu\tilde{E}/\gamma\theta) \sim 10^4$ sec^{-1}, $\eta \sim \frac{1}{\tilde{E}}\sqrt{K/\epsilon_a} \sim 10^{-5}$ m, $b = d/\eta \sim 10$, and $\omega_{ext} \sim 10^3$ sec^{-1}. In fact, quantities γ, K, and ϵ_a are not known exactly, but they can be estimated from the experiments by the proper choice of parameters a and b for the best fitting.

The study of dependence $I(\omega)$ at very low frequencies meets some difficulties related to the necessity of the proper choice of instrument constant t_0 mentioned above. If parameter t_0 has an occasional value, i.e., the upper integration limit in Eqs. (23) and (24) can fluctuate, then the observed scattering intensity can have occasional jumps at very low frequencies.

Another question, related to the low frequency behavior of quantity $I(\omega)$, arises when we study very thin films (see Fig. 3). In this case, the maximum intensity is almost absent at $\omega \sim a/b \sim (a\eta/d) \Rightarrow \infty$, but expansions (25) and (26) stay valid at $\omega \gg a$, i.e., even at sufficiently low frequencies if field $\tilde{E}$ is not too strong. Therefore, in such a case, the frequency range, in which laws (25) and (26) are valid (at fixed t_0, these laws take the form of const$\times\omega^{-2}$), is expanded, and one can observe the increase of scattering intensity at frequency decreasing even at $\omega \ll (a/b)$.

V. CONCLUSIONS

The presented model is based on the assumption that the films consist of the exterior layers, where the vector order parameter $\vec{\xi}$ is spontaneously oriented due the effects of the dipolar interaction decribed in [9,10], and the interior layers where the conic Sm-C^* spiral with axes perpendicular to the layers is suppressed. The contribution from the Goldstone mode to the light scattering is therefore neglected. The kink mechanism determines the reorientation of the director field in the interior layers of the films. The director reorientation starts from the induction of the kink on the boundary of the exterior anisotropic layer (in thick films) or on the boundaries of the specific domains (in thin films), which then propagates with a certain velocity perpendicular to the films surface in the case on thick films or parallel to it in thin films. When the film thickness is comparable with the thickness of the ordered exterior region, the kink mechanism does not work generally. The films dynamics is qualitatively changed and other mechanisms have to be considered. The model of kink switching has given a good qualitative correlation with the experiment for the film thicknesses $N \geq 120$ and enabled the estimation of until unknown material parameters: viscosity and polar anisotropy.

ACKNOWLEDGMENTS

The authors are grateful to Professor H. Stegemeyer for discussions and cooperation; Dr. U. Hoffmann for the development of the computer program; S. Astafiev for the technical assistance; and the Deutsche Forschungsgemeinschaft (Germany), INTAS (European Commission), and Russian Foundation for the Fundamental Research for financial support.

[1] P. Pieranski *et al.*, Physica A **194**, 364 (1993).
[2] C.C. Huang and T. Stoebe, Adv. Phys. **42**, 343 (1993).
[3] E. Demikhov, Europhys. Lett. **25**, 259 (1994).
[4] E. Demikhov and H. Stegemeyer, Liq. Cryst. **18**, 37 (1995).
[5] E.I. Demikhov, Phys. Rev. E **51**, 12 (1995).
[6] E.I. Demikhov and S.A. Pikin, Pis'ma Zh. Eksp. Teor. Fiz. **61**, 666 (1995) [JETP Lett. **61**, 686 (1995)].
[7] E.I. Demikhov, E. Hoffmann, H. Stegemeyer, S.A. Pikin, and A. Strigazzi, Phys. Rev. E, **51**, 5954 (1995).
[8] E.I. Demikhov, Mol. Cryst. Liq. Cryst. **265**, 403 (1995).
[9] R.A. Pelcovits and B.I. Halperin, Phys. Rev. B **19**, 4614 (1979).
[10] S.A. Pikin, *Strukturnye Prevrashenija v Zhidkih Kristal-*

lah (Nauka, Moscow, 1981) [English translation: *Structural Transformations in Liquid Crystals* (Gordon and Breach Science Publishers, New York, 1991)].
[11] P. Schiller, G. Pelzl, and D. Demus, Liq. Cryst. **2**, 21 (1987).
[12] S. A. Pikin, Mol. Cryst. Liq. Cryst. **179** 201 (1990).
[13] S.A. Pikin, Ferroelectrics **117** 197 (1991).
[14] Ch. Bahr and G. Heppke, Mol. Cryst. Liq. Cryst. **148**, 29 (1987).
[15] Ch. Bahr and D. Fliegner, Phys. Rev. A **46**, 7657 (1992).
[16] I. Kraus, P. Pieranski, E. Demikhov, and H. Stegemeyer, Phys. Rev. E **48**, 1916 (1993).